Nano Res (2010) 3: 459–471
DOI 10.1007/s12274-010-0005-9
Research Article

Interplay of Adsorbate–Adsorbate and Adsorbate–Substrate Interactions in Self-Assembled Molecular Surface Nanostructures

Joachim Schnadt[1,2] (✉), Wei Xu[1,3], Ronnie T. Vang[1], Jan Knudsen[1], Zheshen Li[4], Erik Lægsgaard[1], and Flemming Besenbacher[1]

[1] Interdisciplinary Nanoscience Center, iNANO, and Department of Physics and Astronomy, Aarhus University, Building 1521, Ny Munkegade, 8000 Aarhus C, Denmark
[2] Division of Synchrotron Radiation Research, Department of Physics, Lund University, Box 118, 221 00 Lund, Sweden
[3] Shanghai Key Laboratory for Metallic Functional Materials, Key Laboratory for Advanced Civil Engineering Materials (Ministry of Education), College of Materials Science and Engineering, Tongji University, 1239 Si Ping Road, Shanghai 200092, China
[4] Institute for Storage Ring Facilities, Aarhus University, Building 1525, Ny Munkegade, 8000 Aarhus C, Denmark

Received: 8 February 2010 / Revised: 29 April 2010 / Accepted: 29 April 2010

ABSTRACT

The adsorption of 2,6-naphthalenedicarboxylic acid (NDCA) molecules on the Ag(110), Cu(110), and Ag(111) surfaces at room temperature has been studied by means of scanning tunnelling microscopy (STM). Further supporting results were obtained using X-ray photoelectron spectroscopy (XPS) and soft X-ray absorption spectroscopy (XAS). On the Ag(110) support, which had an average terrace width of only 15 nm, the NDCA molecules form extended one-dimensional (1-D) assemblies, which are oriented perpendicular to the step edges and have lengths of several hundred nanometres. This shows that the assemblies have a large tolerance to monatomic surface steps on the Ag(110) surface. The observed behaviour is explained in terms of strong intermolecular hydrogen bonding and a strong surface-mediated directionality, assisted by a sufficient degree of molecular backbone flexibility. In contrast, the same kind of step-edge crossing is not observed when the molecules are adsorbed on the isotropic Ag(111) or more reactive Cu(110) surfaces. On Ag(111), similar 1-D assemblies are formed to those on Ag(110), but they are oriented along the step edges. On Cu(110), the carboxylic groups of NDCA are deprotonated and form covalent bonds to the surface, a situation which is also achieved on Ag(110) by annealing to 200 °C. These results show that the formation of particular self-assembled molecular nanostructures depends significantly on a subtle balance between the adsorbate–adsorbate and adsorbate–substrate interactions and that kinetic factors play an important role.

KEYWORDS

Molecular self-assembly, hydrogen bonding, scanning tunnelling microscopy, X-ray photoelectron spectroscopy

1. Introduction

The ultimate goal of supramolecular chemistry—whether applied to bulk materials or to structures at surfaces—is, in a bottom-up approach, to deliberately and reproducibly grow extended molecular assemblies with specific and desired structural, chemical, physical, and functional properties [1]. It is of the utmost

Address correspondence to joachim.schnadt@sljus.lu.se

importance to understand the underlying factors which lead to the formation of certain molecular nanostructures in order to reach the goal of achieving the synthesis and growth of tailored molecular self-assembled nanostructures. During the past decades supramolecular chemistry has been developed extensively and is approaching a stage at which it is possible to control the growth of 3-D nanostructures [2]. However, due to the physical and chemical complexity of 2-D surfaces, the structure of surface-confined 2-D molecular assemblies is much more difficult to steer and control. While tremendous advances have been made in the field of surface supramolecular chemistry [3–12], investigations have often been performed for highly idealised systems of flat metal surfaces under clean and well controlled ultrahigh vacuum (UHV) conditions. Such extreme conditions offer the possibility to improve our basic understanding of the very details of molecular assembly formation and properties, but, of course, these conditions are far from those in many nanotechnological applications (such as in the area of biosensing), not least in terms of the pressure and the structural complexity of the substrates. In the field of catalysis, the "gaps" between the conditions of the UHV model system and realistic industrial conditions have been termed the pressure and materials gaps, respectively, and these terms also provide a valid description within the area of surface supramolecular chemistry. Ways to circumvent the gaps, while maintaining control of the experimental parameters, include raising the pressure in a very controlled way [13] and/or introducing surfaces of increased complexity such as stepped surfaces [14] or metal clusters deposited on flat surfaces [15]. In a previous publication [16] we have used the latter approach and studied the formation of 1-D supramolecular assemblies on a stepped Ag(110) surface. These assemblies, which are formed from 2,6-naphthalenedicarboxylic acid (NDCA, Fig. 1) and which are intermolecularly linked by cyclic hydrogen bonds between the carboxylic functional groups, were shown to be able to cross single-atomic step edges, as illustrated in Fig. 2. This behaviour enables the 1-D structures to extend to mesoscopic length scales, in spite of the stepped character of the surface. We found that the prime factors leading to the step-crossing ability of the assemblies are a strong

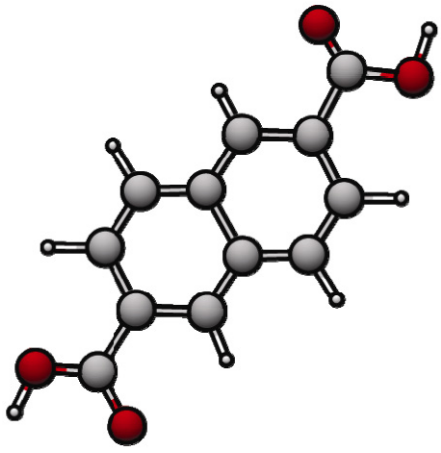

Figure 1 Molecular structure of 2,6-naphthalenedicarboxylic acid. Grey spheres are carbon atoms, red spheres oxygen, and white spheres hydrogen

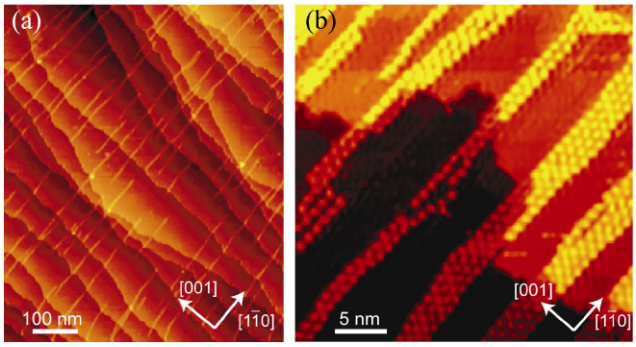

Figure 2 STM images illustrating the step-edge crossing of the NDCA 1-D chains: (a) Submonolayer (0.1 ML) of NDCA on Ag(110), 620 nm × 700 nm, –0.39 nA, –221 mV; (b) ~0.37 ML, 32.5 nm × 32.5 nm, –0.1 nA, –442 mV

intermolecular hydrogen bond motif in conjunction with a distinct surface-mediated directionality and a sufficient flexibility of the molecular backbone [16]. In this paper we provide further experimental details of our studies of NDCA on Ag(110) and present comparative investigations of the adsorption of NDCA on Ag(111) and Cu(110) surfaces.

2. Experimental

The scanning tunnelling microscope (STM) experiments were performed using the home-built Aarhus STM [17] mounted on two different UHV chambers with base pressures of 1×10^{-10} Torr. The X-ray photoelectron spectroscopy (XPS) and X-ray absorption spectroscopy experiments were carried out at the SX700 beam line

of the Danish synchrotron radiation facility ASTRID [18]. The end station of this beam line consists of a UHV chamber (base pressure 1×10^{-10} Torr) fitted with a VG-CLAM2 electron energy analyzer. The X-ray absorption spectra were recorded in Auger yield mode at a photon energy resolution of approximately 0.2 eV. In order to account for the variation of the photon flux with photon energy, the spectra were divided by spectra measured on the clean sample surface.

The surfaces of the Ag and Cu samples were cleaned by repeated cycles of Ar^+ or Ne^+ sputtering and annealing: the silver surfaces were sputtered for 10 min using 0.6 keV ions and the Cu(110) surface for 20 min using 1.0 keV ions, and the annealing temperatures were 480 ˚C applied for 5 to 10 min, 300 ˚C for 10 min, and 520 to 540 ˚C for 20 to 25 min in the case of the Ag(110), Ag(111), and Cu(110) surfaces, respectively. After the cycles, STM or XPS measurements were performed to ensure that the samples were clean. 2,6-NDCA was sublimated onto the clean samples at room temperature (RT) from a home-built sublimation doser with the molecular powder held at temperatures between 260 and 420 ˚C. Cooling the scanning tunnelling microscope to liquid nitrogen temperatures facilitated obtaining high-quality STM images and, thus, most of the STM images were recorded at low temperature. Test experiments carried out at RT gave identical results.

3. Results

3.1 STM results

STM images of the most commonly observed submonolayer adsorption structures of NDCA on the Ag(110), Ag(111), and Cu(110) surfaces are presented in Figs. 2–5. The STM results for Ag(110) in Figs. 2, 3(a) and 3(b) were obtained using NDCA sublimated onto a Ag(110) surface at room temperature. The large-scale STM image in Fig. 2(a) shows that

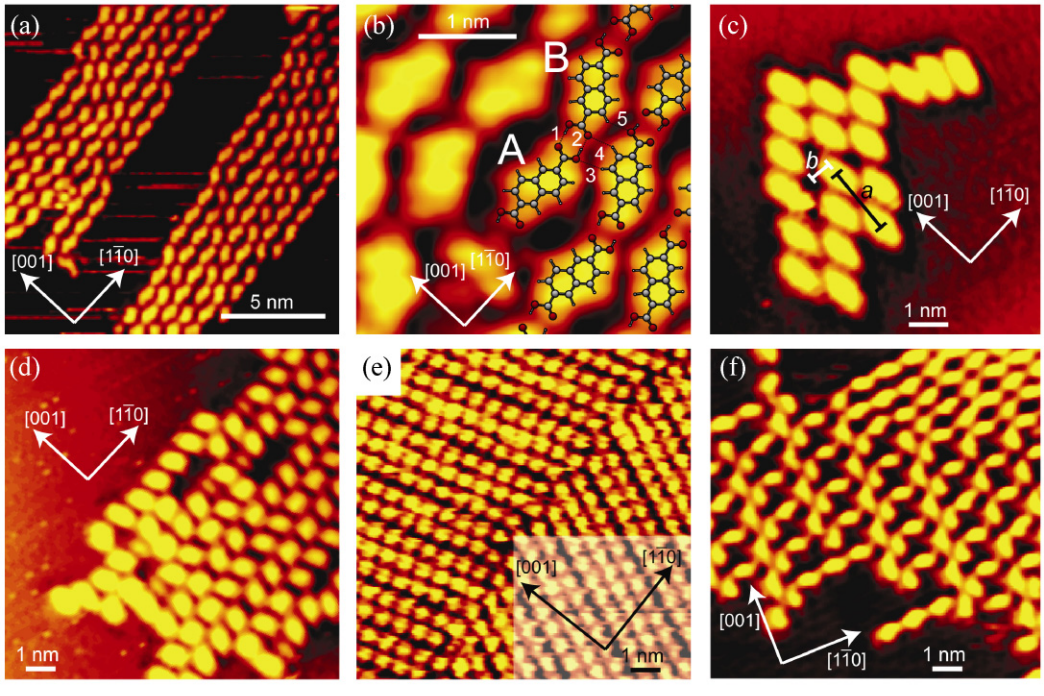

Figure 3 STM images of adsorption of NDCA on Ag(110). Room temperature adsorption on Ag(110), cf. also Fig. 1: (a) 16 nm × 16 nm, 0.2 nA, 186 mV; (b) 3.4 nm × 3.4 nm, –0.26 nA, –186 mV. The arabic numbers in (b) indicate primary (1 and 2) and secondary (3 to 5) hydrogen bonds, respectively, while the capital letters indicate the two experimentally observed terrace species. Submonolayer NDCA/Ag(110) annealed to 200 ˚C for 10 min after deposition: (c) 8.4 nm × 8.4 nm, –0.17 nA, –1051 mV; (d) 11.2 nm × 11.2 nm, –0.16 nA, –1051 mV. (e) Monolayer NDCA/Ag(110) formed by deposition of multilayer NDCA on Ag(110) followed by annealing to 200 ˚C, 11.2 nm × 11.2 nm, –0.54 nA, –39.1 mV; (f) Submonolayer NDCA on Ag(110) heated to approximately 50 ˚C during deposition, 11.2 nm × 11.2 nm, –0.5 nA, –1051 mV

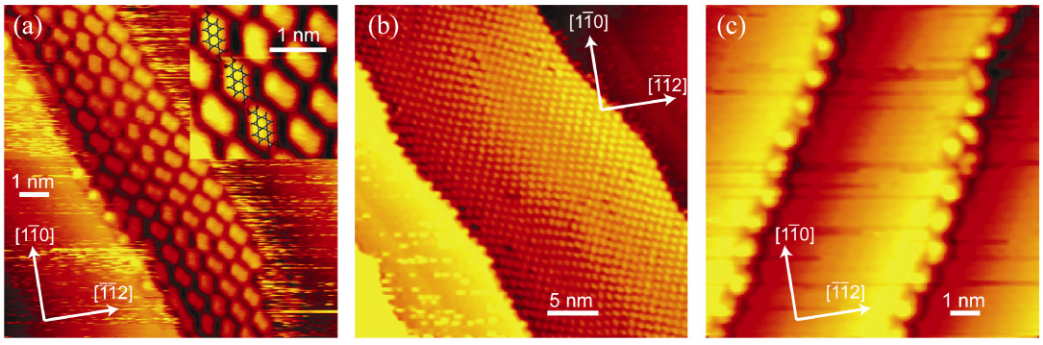

Figure 4 STM images of NDCA adsorption on Ag(111): (a) 11.2 nm × 11.2 nm (inset 2.6 nm × 2.6 nm), –0.09 nA, –1051 mV; (b) 32.5 nm × 32.5 nm, –0.11 nA, –1250 mV; (c) NDCA/Ag(111) after annealing the room temperature structure to 100 ˚C for 10 min: 11.2 nm × 11.2 nm, –0.13 nA, –1051 mV

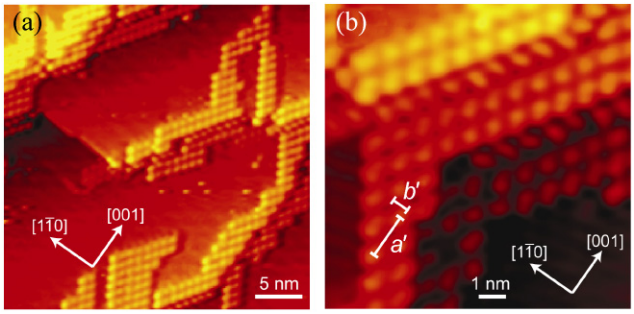

Figure 5 STM images of adsorption of NDCA/Cu(110) at room temperature: (a) 32.5 nm × 32.5 nm, –0.43 nA, –625 mV; (b) 11.2 nm × 11.2 nm, –0.33 nA, –625 mV

the molecules self-assemble in quasi-one-dimensional chains (1-D chains) over large distances on the nanometre scale. The lengths of the 1-D chains of molecules extend up to the micrometre range. Since the surface is quite stepped, the long lengths of the 1-D chains imply that most of them must cross the monatomic steps of the surface. For example, more than 90% of all 1-D chains in Fig. 2(a) cross one or more step edges. A zoom-in STM image of 1-D chains crossing a step edge is found in Fig. 2(b). Now considering the molecular-scale details of the 1-D chains on terraces of the Ag(110) surface, it is seen from Fig. 3(a) that the NDCA molecules are aligned with their molecular axes approximately along the [1$\bar{1}$0] direction, i.e., along the close-packed rows of Ag(110). The individual adsorbate orientations are very similar for all NDCA molecules; however, Fig. 3(a) also shows that there exists some variation in the exact adsorbate geometry, which may be due to the fact that the carboxylic groups can be rotated around the σ bond between the functional group and the naphthalene core. This slight variation in molecular adsorption geometry results in a manifold of different chemical environments for the carboxylic oxygen atoms and intermolecular hydrogen bonds, as will be discussed further below. It can be seen from Fig. 3(b) that one can distinguish between two primary molecule orientations, A and B. An analysis of approximately 100 STM images shows that these two orientations occur in a ratio of 1:2. Our previously published calculations showed that species A is adsorbed on top of the close-packed rows of silver atoms of the Ag(110) substrate [16]. 1-D chains of this species alone are strictly oriented along the [1$\bar{1}$0] direction, and the distance between the adsorbates along this direction is 11.56 Å, which corresponds to four substrate Ag atoms [16]. In the vertical direction, i.e., along the [001] direction, the distance between neighbouring NDCA adsorbates is two rows of close-packed silver atoms, or 8.18 Å. Figure 3(b) shows that the carboxylic groups of adsorbate species B rest on adjacent close-packed silver atom rows and that the napthalene core is thus positioned over a surface trough.

Upon annealing a submonolayer-covered surface, such as shown in Fig. 3(a), to 200 ˚C, the 1-D chains are destabilised and the molecules reorganise into small patches of NDCA adsorbates with their molecular axes rotated by 90˚ and now approximately aligned along the [001] surface direction (Figs. 3(c) and 3(d)). Step-edge crossing is not observed anymore. In Fig. 3(c), two distances between NDCA adsorbates, *a* and *b*, are indicated: *a* is along the [001] substrate direction and 16.9 Å ± 0.5 Å long, while *b* is along [1$\bar{1}$0]

and 5.9 Å ± 0.5 Å long. In terms of distances between neighbouring Ag atoms of the substrate, a is 4.1 ± 0.15 times the distance between adjacent close-packed rows of the substrate, whilst b is 2.0 ± 0.2 times the distance between the Ag atoms in the close-packed rows.

Futhermore, low-temperature annealing of the NDCA/Ag(110) submonolayer preparations was found to result in a modification of the adsorbate structure. Figure 3(f) shows an STM image of an NDCA submonolayer deposited onto a sample kept at approximately 50 °C. We observe a co-existence of the 1-D chain structure in the upper right corner and an additional "ladder" molecular nanostructure in the remaining part of the image. In this ladder structure, one third of the molecules are aligned with their molecular axes along the [001] direction and two thirds with their axes along [1$\bar{1}$0]. The same ladder structure was also observed after annealing surfaces characterised by 1-D chains to temperatures between 50 and 100 °C.

For comparison, it should be noted that the molecular geometries found in full monolayers (MLs) deviate from the molecular geometries observed for both the as-grown and the annealed submonolayers. Monolayers were obtained in two ways: (1) by gradual deposition and, in some cases, subsequent annealing to 200 °C and (2) by annealing a molecular multilayer structure to 200 °C. Figure 3(e) shows an STM image obtained by using the second method. Clearly, both the molecular orientation, distance between NDCA adsorbates, and overall arrangement differ from those observed for the submonolayers.

We now turn to the adsorption of NDCA on Ag(111). The molecular details of the adsorbate geometry after sublimation of the NDCA molecules onto the Ag(111) surface at room-temperature are very similar to those formed by the NDCA molecules on Ag(110) at RT. Again, quasi 1-D chains are observed, as shown in Figs. 4(a) and 4(b). However, the widths of the molecular chains are typically considerably broader on Ag(111) as compared with those of the 1-D chains on the Ag(110) surface. In addition, the chains are aligned along the substrate step edges rather than perpendicular to them as in the Ag(110) case, that is, step-edge crossing is not observed. Upon annealing to 100 °C, most of the NDCA adsorbates are desorbed, with only a single molecule-wide brim left at the lower step edges (Fig. 4(c)). The relatively low desorption temperature for NDCA molecules on the terraces of the Ag(111) surface implies that the molecule–substrate interaction is weaker for the Ag(111) than for the Ag(110) surface.

Finally, the STM image in Fig. 5(a) shows that the RT adsorption structure of NDCA on Cu(110) is quite different from those on the Ag(110) and Ag(111) surfaces. It strongly resembles the structure observed after annealing the low-coverage NDCA/Ag(110) system, with the NDCA molecules forming adsorbate patches, in which the molecules are aligned with the molecular axes along the [001] direction. Along this direction the distance between neighbouring adsorbates, i.e., distance a' in Fig. 5(b), is 16.2 Å ± 0.5 Å, equivalent to 4.5 ± 0.15 times the distance between neighbouring close-packed rows of Cu atoms. The perpendicular distance along the [1$\bar{1}$0] direction (distance b') is 5.8 Å ± 0.5 Å, which corresponds to 2.2 ± 0.2 times the distance between adjacent Cu atoms in the close-packed rows. The degree of order within the patches is considerably higher on the Cu(110) surface than on the Ag(110) surface, and the NDCA molecules tend to decorate the step edges in a well-ordered fashion (Fig. 5(b)).

3.2 XPS results

In Fig. 6, O 1s X-ray photoelectron spectra are shown for NDCA molecules adsorbed on the Ag(110) and Cu(110) surfaces, and the deduced binding energies are listed in Table 1. For the multilayer structure, a symmetric peak is observed (Fig. 6(a)), which is composed of two components of equal weight. The higher binding energy peak corresponds to photoemission from the hydroxyl oxygen of the carboxylic group and the lower binding energy component corresponds to photoemission from the carbonyl oxygen [19]. For a NDCA submonolayer structure on Ag(110) (Fig. 6(b)), the peak initially is also composed of two components. Annealing to 200 °C first for 10 min (Fig. 6(c)) and subsequently for another 10 min (Fig. 6(d)), leads first to the reduction, followed by the disappearance of the higher binding energy component. This kind of modification of the O 1s line shape is typical for a deprotonation reaction of carboxylic groups

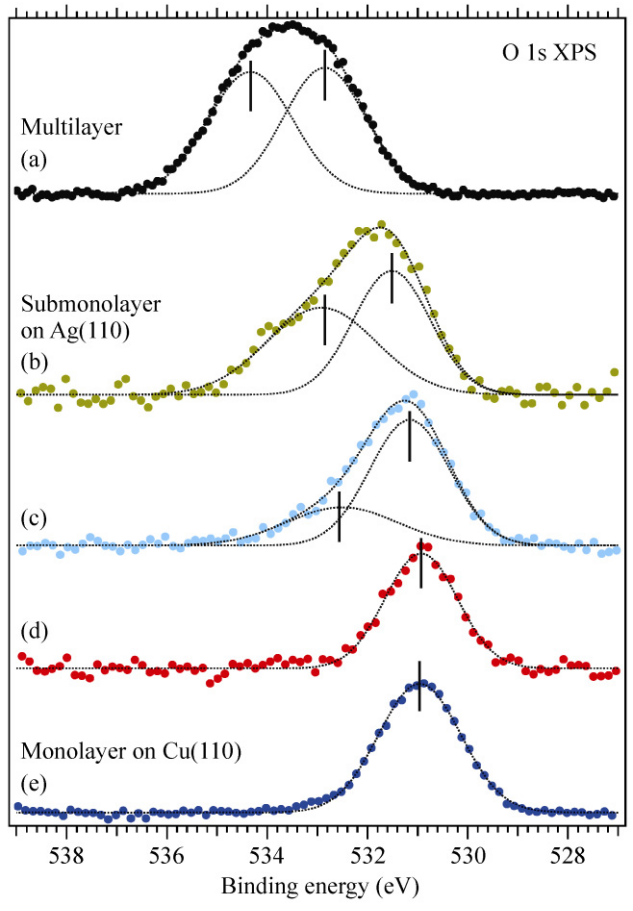

Figure 6 O 1s X-ray photoelectron spectra. (a) obtained for a multilayer of NDCA deposited onto Ag(110) at RT, and (b) for approximately 0.3 ML of NDCA deposited onto Ag(110) at RT. This sample was subsequently annealed to 200 ˚C for 10 min, which resulted in (c). A second 10 min anneal at 200 ˚C yielded (d). (e) XPS spectra for 1 ML of NDCA on Cu(110)

concomitant with the formation of a covalent bond between the substrate and the carboxylate [16, 20]. It can be explained by the presence of two inequivalent oxygen species in the protonated molecule, which are rendered equivalent by deprotonation and bond formation. A priori, one would have expected to observe two components of *similar* widths for the intact molecule, while the O 1s spectrum of the RT preparation in Fig. 6(b) is characterised by two components with equal weights, but different widths. This introduces an asymmetry into the overall shape of the line profiles of the XPS peaks. We will argue below that the adsorbate assembly is characterised by cyclic intramolecular hydrogen bonds between the carboxylic groups of adjacent NDCA molecules. The variation in the adsorbate geometry discussed above will also lead to a variation of the exact hydrogen bond geometry. Since the cyclic hydrogen bonding motif is expected to affect the XPS binding energy of the O 1s hydroxyl peak much more strongly than that of the carbonyl peak [21], the hydroxyl O 1s binding energies will also vary more strongly with the atomic positions and the chemical environment of the oxygen atoms than the carbonyl O 1s binding energies. Hence, the variation in adsorbate geometry is expected to lead to a broadening of the hydroxyl O 1s line, as is observed in the XPS spectrum in Fig. 6(b). Indeed, similar asymmetries of the O 1s line have been observed previously for multilayers of fully protonated carboxylic acids [22]. For these systems it is not the slightly different surface adsorption sites which give rise to the broadening of the hydroxyl O 1s line, but small differences in the chemical environments of the hydroxyl oxygen atoms in the molecular multilayers. Apart from this difference, the cases here and in Ref. [22] exhibit clear parallels. It is also interesting to note that related XPS studies of systems with hydrogen bonds between a donor carboxylic group and a pyridine acceptor have found a much stronger influence of the hydrogen bond on the binding energy of the acceptor N 1s line than on the donor O 1s line [23, 24]. This contrasts with the observation made here and the observations and calculations in Refs. [21, 25, 26] for hydrogen-bonded carboxylic acid dimers, where it was found that the O 1s binding energy of the donor oxygen is considerably more strongly influenced by the hydrogen bond than that of the acceptor oxygen. Since the behaviour observed here closely matches that found in the previous studies on carboxylic acid dimers, the shape of the O 1s spectrum is taken as proof of the intactness of the NDCA molecules on Ag(110) with no deprotonation of the carboxylic groups occurring at RT.

The O 1s spectrum for the annealed NDCA/Ag(110) system, with covalent bonds between the carboxylic groups and the substrate (Fig. 6(d)) is very similar to the corresponding spectrum for NDCA/Cu(110) (Fig. 6(e)). Thus, the NDCA adsorbates are completely deprotonated upon RT adsorption on the Cu(110) surface, and covalent bonds are formed between the carboxylate and the copper substrate.

Table 1 O 1s XPS binding energies deduced from the spectra in Fig. 6. Due to the lack of an observable Fermi energy only relative values are provided for the multilayer data, while the reference for the other energies is the substrate Fermi level. The component binding energies are derived from fitting the signals by two Gaussians. For the monolayer and non-annealed NDCA/Ag(110) the two Gaussians representing the hydroxyl and carbonyl O 1s signals were constrained to have the same area

	O 1s	
	Hydroxyl	Carbonyl
(a) Multilayer	Δ = 1.48 eV ± 0.05 eV	
(b) RT sub-ML on Ag(110)	532.91 eV ± 0.05 eV	531.51 eV ± 0.05 eV
	Δ = 1.40 eV ± 0.07 eV	
(c) Sub-ML on Ag(110) annealed to 200 °C for 10 min	532.56 eV ± 0.05 eV	531.16 eV ± 0.05 eV
	Δ = 1.40 eV ± 0.07 eV	
(d) Sub-ML on Ag(110) annealed to 200 °C for 20 min	530.93 eV ± 0.05 eV	
(e) RT sub-ML on Cu(110)	530.96 eV ± 0.05 eV	

3.3 XAS results

For the NDCA/Ag(110) system prepared at RT C 1s X-ray absorption spectra were acquired at normal and 55° grazing X-ray incidence. The spectra, divided by a virgin spectrum recorded on the clean substrate, are displayed in Fig. 7. Since XAS is an integrating method, the spectra represent an average over the geometries of all probed NDCA adsorbates. From the step density we estimate that approximately 5% of all molecules are adsorbed adjacent to the step edges, i.e., 2.5% at the upper and 2.5% at the lower step edges. Due to this low number, XAS is not particularly sensitive to changes in the adsorption geometry between the terrace adsorbates and adsorbates at the step edges. In particular, moderate changes of the orientation such as an upwards or downwards bend of the adsorbates by a few degrees are not discernible in the spectra. The XAS results should therefore be considered to be representative for the terrace NDCA adsorbates only.

The asymmetric low-energy peak in the X-ray absorption spectrum in Fig. 7 at around 285 eV is attributed to excitations from the naphthalene C 1s levels to the LUMO [27], while the higher energy peak at around 288 eV stems primarily from excitations

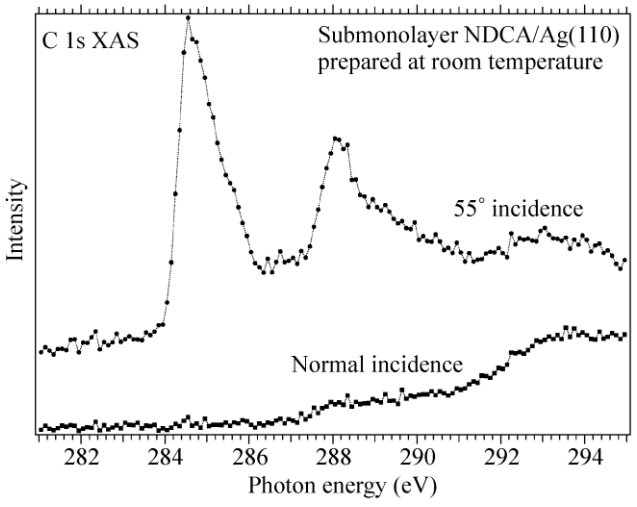

Figure 7 C 1s X-ray absorption spectra for the same non-annealed submonolayer NDCA/Ag(110) preparation as in Fig. 6(b). An intensity offset was applied to the spectra for reasons of presentation. The incidence angle was measured from the surface normal

of electrons from the carboxylic C 1s level into the LUMO [28] plus a possible admixture of further excitations on the naphthalene part of the molecule [27]. The main part of the intensity at higher energies is attributed to the excitation of a σ^* resonance.

The low-energy π^* resonances observed at 55° incidence are completely absent for normal incidence. This finding indicates a perfectly flat adsorbate geometry of the NDCA molecules on the Ag(110) terraces, which is in good agreement with the appearance of the NDCA molecules in the STM image in Fig. 3(a). Since the STM appearance of the molecules is the same for all preparations, it is concluded that the molecules lie flat on the terraces in all investigated systems.

4. Discussion

4.1 Non-covalent adsorption of NDCA on substrate terraces: Ag(110)

The XPS and XAS results presented above show that on the Ag(110) surface the NDCA molecules remain intact after the RT deposition and that they lie flat on the surface. From this we infer that the NDCA–substrate bond is non-covalent. Furthermore, the STM images suggest that head-to-head hydrogen bonding is responsible for the intermolecular bonding within

the 1-D-chains along the [1$\bar{1}$0] direction. If we first concentrate on the NDCA adsorbates on the terraces, the notion of a hydrogen-bonded assembly is consistent with previously published DFT calculations [16]. The calculations were performed for a number of different NDCA geometries with different rotation angles to the [1$\bar{1}$0] axis of the substrate. It was found that the most stable NDCA assembly on the Ag(110) terraces is characterised by NDCA adsorbates which are aligned with their molecular axes along the [1$\bar{1}$0] direction and with cyclic hydrogen bonds between the carboxylic groups of the NDCA molecules. This adsorption geometry agrees very well with the experimentally observed adsorption geometry of species A depicted in the STM images in Fig. 3(b). The distance along the [1$\bar{1}$0] direction between two adsorbates of species A is 11.56 Å measured between the centres of the molecules, which is in very good agreement with the length of the NDCA molecule (11.64 Å) determined from powder diffraction measurements [29] (note that the formation of a cyclic hydrogen bond motif between the carboxylic groups of neighbouring NDCA adsorbates implies that the centre-to-centre distance between the two molecules should be essentially equal to the length of a single molecule). The DFT binding energy for the hydrogen-bonded geometry of species A was found to be 1.20 eV/molecule, of which 0.9 eV can be attributed to the effect of hydrogen bonding. Less than 0.1 eV is due to intermolecular interactions along [001] and thus only around 0.2 eV is associated with the substrate–adsorbate bond. Since DFT calculations do not give a proper account of dispersion interactions, the latter value may be put into perspective by making a comparison with a recent DFT calculation of the parallel adsorption of pyridine on Ag(110) [30]. In this calculation the van der Waals interactions were taken into account in a semiempirical way and it was found that the dispersion forces stabilise the adsorption by approximately 0.3 eV. Since naphthalene is around twice as large as pyridine, one may thus tentatively expect the stabilisation energy to be around 0.5 to 0.6 eV per molecule in the present case. Together with the 0.2 eV from our previous DFT calculations, this indicates that the substrate–adsorbate interaction is comparable in size (ca. 0.8 eV) to the hydrogen bond interaction of 0.9 eV.

The experimental observation of the other terrace species B, (Fig. 3(b)), could not be further confirmed by the DFT calculations. In terms of calculational modelling, species B is different from species A, in that an overlayer structure of species B alone is incommensurate with the Ag(110) substrate, which renders a periodic supercell calculation containing both the overlayer and substrate impossible. Nevertheless, it is clear that the adsorption energy of species B must be very similar to that of species A, since both species are observed together with an approximate abundance ratio of 2:1 (A:B). Using a Boltzmann distribution argument, the difference in adsorption energies is found to be only ~0.02 eV, which is less than, but close to, kT at room temperature.

It is instructive to try to determine the experimentally observed intermolecular atomic distances in Fig. 3(b). The bond lengths in Table 2 were derived from the model in Fig. 3(b) and thus rely on the independent length calibration of the STM image. Applying a simple length criterion for the classification of hydrogen bonds [31], the intermolecular bonds labelled 1 and 2 in Fig. 3(b) fall into the range of moderately strong to strong hydrogen bonds. Using the same criterion, it also appears that there exist weak hydrogen bonds in the lateral direction, namely along lines 3, 4, and 5 in Fig. 3(b). These weak hydrogen bonds will contribute to the stability of the molecular assembly. Furthermore, their existence provides a reasonable explanation for the fact that the experimentally observed 1-D chains almost always consist of several head-to-head hydrogen-bonded rows of NDCA adsorbates. Only very rarely were short pieces of single rows of NDCA molecules observed in the STM images: an analysis of around 100 STM images showed that approximately 5% of the 1-D chains contained short sections of chains with a single-molecule breadth only. Figure 2(b) shows

Table 2 Lengths of the indicated distances in Fig. 3(b)

Bond	Experimental bond length (±10%)
1	1.5 Å
2	1.6 Å
3	2.8 Å
4	2.9 Å
5	2.9 Å

one of the few STM images where such a single-molecule chain was observed. The single-molecule chains were typically found at the end of broader 1-D chains, and they were never longer than a couple of molecules; the total length of these sections was less than 1% of the total length of the 1-D chains. Completely free-standing single-molecule 1-D chains were observed in not more than three cases (out of several hundred STM images).

4.2 Room temperature adsorption of NDCA on Ag(110): Adsorbates at the step edges

The most prominent characteristic of the NDCA/Ag(110) system is the formation of 1-D chains with lengths up to the micrometre regime, which even extend over the monatomic steps of the substrate (Fig. 2(a)). In our previous publication [16], we presented DFT calculations of a number of different NDCA arrangements at the step edges, aimed at understanding the details of the molecular arrangement. In these calculations, the energy of the cyclic hydrogen bond motif was found to be 0.92 eV for the most stable geometry of a non-covalently bonded NDCA dimer at a monatomic step edge. This energy is significantly smaller than the energy of the same adsorption motif for a terrace assembly, which is 1.20 eV. The reduction in energy probably stems primarily from a disturbance of the optimum hydrogen bond geometry. At the step edge the planarity of the carboxylic groups cannot be fully maintained, which implies an energetically less favourable adsorption configuration in terms of both the hydrogen bond energy and the energy of the covalent bonds of the carboxylic groups. In addition, the dispersion energy contribution from the NDCA adsorbate–substrate interaction is lower for NDCA adsorption at the lower step edge due to the larger distance of the NDCA body from the substrate as compared to the distance of the NDCA molecule from the substrate in the ideal terrace geometry. The calculations also showed a slight 12° upward bend of the NDCA molecules on the lower terraces. This bend does not significantly alter any of the bond geometries and thus does not contribute to the lowering of the adsorption energy.

A breaking of the double hydrogen bond between the lower and upper terrace NDCA adsorbates was found to imply an additional considerable reduction of the NDCA adsorption energy (ΔE ~0.3 eV) [16]. Thus, the picture which emerges is that the monatomic step edges partially prohibit the formation of an optimal NDCA–NDCA bond. Nevertheless, it is energetically far more favourable for the NDCA adsorbates to continue the terrace 1-D chains over the step edges rather than leaving the ends of the 1-D chain open. It should be noted, however, that the difference in energy of the terrace and step edge NDCA adsorption geometries as well the anisotropy of the substrate directions lead to a window of kinetically preferred values of substrate temperature and adsorbate flux for the formation of macroscopic 1-D NDCA assemblies, which indeed do cross the step edges [32].

4.3 Non-covalent adsorption of NDCA on substrate terraces: Ag(111)

As already pointed out above in the Results section, the STM appearance of the NDCA assembly on Ag(111) is very similar to that on Ag(110), cf. Figs. 4(a) and 4(b), and the primary geometrical motif of head-to-head bonded NDCA adsorbates is also found in the case of Ag(111). This is qualitatively confirmed by superposing an overlayer composed of NDCA species A as found for the Ag(110) surface onto the STM image, as shown in the inset of Fig. 4(a). The adsorbate–substrate interaction on Ag(110) is due to pure van der Waals interactions. In view of the reduced chemical reactivity of the close-packed Ag(111) surface in comparison to the more open Ag(110) surface, this must be true also for the NDCA–Ag(111) interaction. The annealing experiment, the result of which is shown in Fig. 4(c), confirms this picture—all terrace NDCA adsorbates desorb before any decomposition reaction and covalent bond formation to the substrate can occur. As will be discussed below, this is in contrast to the finding for the more reactive Ag(110) surface. Hence, as expected, the NDCA–substrate bond is even weaker on Ag(111) than on Ag(110), but, both cases are representatives of a weak dispersion force type of interaction.

A comparison of the NDCA adsorption structures on the Ag(111) and Ag(110) surfaces clarifies the role of the substrate anisotropy for the formation of mesoscale 1-D self-assemblies, which are able to cross

step edges. In both cases the cost of step-edge crossing should be approximately the same. In the Ag(110) case, the cost is compensated for by the gain which originates from the fact that the 1-D chains orient themselves along the [1$\bar{1}$0] direction. This effect is absent on the Ag(111) surface and, thus, step crossing does not occur in this case.

4.4 Covalent bonding

The XPS data in Fig. 6 show that the carboxylic groups of the NDCA molecules are deprotonated upon RT deposition on Cu(110) and upon annealing of the RT adsorption structure on Ag(110). The STM results also show that the covalently bonded adsorbates lie flat on the surface, and that their molecular axes are aligned along the [001] direction. The alignment is excellent for Cu(110), while it is less perfect for the Ag(110) surface. The difference can probably be attributed to a better match between the periodicity of the overlayer structure and that of the substrate in the case of the Cu(110) surface. For both surfaces the distance along the [1$\bar{1}$0] direction between the molecular rows is around twice the distance between the atoms of the close-packed rows. This distance is relatively small, but does not imply any steric problems due to the staggered arrangement of the molecules. We speculate that it arises from the formation of intermolecular hydrogen bonds. The distance between neighbouring NDCA adsorbates in the [001] direction, around four times the lattice constant for Ag(110) and 4.5 times the lattice constant for Cu(110), is too large for any sizeable direct interaction between the molecules to occur. It is well known that mobile substrate adatoms may play an important role in the structure of molecular overlayers, and such mobile adatoms are readily available on both the Ag(110) and Cu(110) surfaces at RT [33, 34]. In particular, the incorporation of Cu adatoms into supramolecular networks has been reported many times [35–40]. We therefore speculate that adatoms are responsible for the intermolecular interaction along the [001] direction, at least in the case of the Cu(110) surface. The lower degree of molecular ordering in the case of the annealed Ag(110) surface suggests that the mechanism of network formation might be different in this case. Without providing any detailed atomic model of the adsorption geometry in these two cases, we can state that the overall adsorption behaviour is very similar to that of trimesic acid (benzene-1,3,5-tricarboxylic acid) on Cu(110) [40], but contrasts with the upright geometry of formic [41] and benzoic acid [42] on the Cu(110) surface. The reason is, of course, that the gain of forming a second covalent bond to the substrate more than outweighs the loss inflicted by the less favourable geometry of the substrate bond.

Considering now the adsorption energies of NDCA on the Cu(110) and annealed Ag(110) surfaces, we note that it may be expected that the covalent bonds between the NDCA adsorbates and the surfaces are similar to those found for formic and benzoic acid [41, 42]. The energy of a single carboxylate–substrate bond can be expected to be several eVs. For example, the adsorption energies of formate and benzoate on Cu surfaces in the presence or absence of Cu adatoms have been calculated by DFT to lie within the range of approximately 3 to 4 eV [43–45]. Somewhat lower, but still comparable, adsorption energies of around 2.5 to 3.5 eV have been found for the adsorption of formate on Ag surfaces [44, 46]. For NDCA adsorbates with the possibility of forming two covalent carboxylate–substrate bonds, one thus would expect adsorption energies of around 6 to 8 eV for the Cu(110) and 5 to 7 eV for the Ag(110) surface. Even though these values are probably reduced by the less favourable carboxylate geometry of a lying-down adsorbate as compared to that of a standing-up formate or benzoate, the adsorption energy of a covalently bonded NDCA adsorbate on the Ag(110) surface is still expected to be much higher than that of the non-covalent arrangement observed at room temperature. Hence, the observation of fully intact NDCA molecules on Ag(110) at RT is the result of a kinetic hindrance towards deprotonation.

The ladder structure formed from NDCA–Ag(110) shown in Fig. 3(f) appears at substrate temperatures during sublimation which are only slightly higher than RT. It is not evident whether in this structure a fraction of the NDCA adsorbates or, alternatively, a fraction of the carboxylic groups of the adsorbates is deprotonated, and whether mobile adatoms play

any role. Irrespective of these open questions, the appearance of the ladder structure indicates that the kinetic hindrance, which keeps the 1-D chains in shape, is small.

5. Conclusions

We have studied the adsorption of NDCA molecules on three different substrates, Ag(110), Ag(111), and Cu(110), and the influence of the annealing temperature on the adsorption structure. The kind of selfassembled nanostructure that is formed is found to result from a complex interplay between the adsorbate–substrate and adsorbate–adsorbate interactions. Hydrogen bonding and also van der Waals interactions play important roles in determining the exact arrangement of the adsorbate molecules in submonolayer and monolayer structures. The adsorbate–substrate interaction, which is different for the different surfaces, is decisive in determining which arrangement is favoured. The (110) surfaces—in contrast to the (111) surfaces—are characterised by a strong anisotropic corrugation of the surface potential. In the limit of a purely dispersion-type adsorbate–substrate interaction, the anisotropy leads to a strongly directional templating effect. This effect is modified for covalently bonded adsorbates, which can be produced on both the Ag(110) and Cu(110) surfaces by a deprotonation reaction of the carboxylic groups. For the Cu(110) surface this reaction occurs at RT, which is the sample temperature during NDCA sublimation, while it is kinetically hindered for the Ag(110) surface. In the latter case slight annealing to temperatures between 50 and 200 °C is required to achieve a partial or full deprotonation of the NDCA molecules.

Acknowledgements

Eva Rauls is acknowledged for discussions and for providing the drawings of the NDCA molecules in Figs. 1 and 2. J. S. acknowledges funding from the European Commission through a Marie Curie Intra-European Fellowship. Funding from the Swedish Research Council (VR) is gratefully acknowledged.

References

[1] Lehn, J. M. Toward self-organization of complex matter. *Science* **2002**, *295*, 2400–2403.

[2] Ariga, K.; Kunitake, T. *Supramolecular Chemistry—Fundamentals and Applications;* Springer: Berlin, 2006.

[3] Barth, J. V.; Costantini, G.; Kern, K. Engineering atomic and molecular nanostructures at surfaces. *Nature* **2005**, *437*, 671–679.

[4] Stepanow, S.; Lin, N.; Barth, J. V. Modular assembly of low-dimensional coordination architectures on metal surfaces. *J. Phys.: Condens. Matter* **2008**, *20*, 184002.

[5] Barth, J. V. Molecular architectonic on metal surfaces. *Annu. Rev. Phys. Chem.* **2007**, *58*, 375–407.

[6] Fichou, D. Structural order in conjugated oligothiophenes and its implications on opto-electronic devices. *J. Mater. Chem.* **2000**, *10*, 571–588.

[7] Barlow, S. M.; Raval, R. Complex organic molecules at metal surfaces: Bonding, organisation and chirality. *Surf. Sci. Rep.* **2003**, *50*, 201–341.

[8] Rosei, F.; Schunack, M.; Naitoh, Y.; Jiang, P.; Gourdon, A.; Lægsgaard, E.; Stensgaard, I.; Joachim, C.; Besenbacher, F. Properties of large organic molecules on metal surfaces. *Prog. Surf. Sci.* **2003**, *71*, 95–146.

[9] Cicoira, F.; Santato, C.; Rosei, F. Two-dimensional nanotemplates as surface cues for the controlled assembly of organic molecules. *Top. Curr. Chem.* **2008**, *285*, 203–267.

[10] Samorì, P. Exploring supramolecular interactions and architectures by scanning force microscopies. *Chem. Soc. Rev.* **2005**, *34*, 551–561.

[11] Liang, H.; He, Y.; Ye, Y. C.; Xu, X. G.; Cheng, F.; Sun, W.; Shao, X.; Wang, Y. F.; Li, J. L.; Wu, K. Two-dimensional molecular porous networks constructed by surface assembling. *Coord. Chem. Rev.* **2009**, *253*, 2959–2979.

[12] Bonifazi, D.; Mohnani, S.; Llanes-Pallas, A. Supramolecular chemistry at interfaces: Molecular recognition on nano-patterned porous surfaces. *Chem. Eur. J.* **2009**, *15*, 7004–7025.

[13] Vang, R. T.; Lægsgaard, E.; Besenbacher, F. Bridging the pressure gap in model systems for heterogeneous catalysis with high-pressure scanning tunneling microscopy. *Phys.*

Chem. Chem. Phys. **2007**, *9*, 3460–3469.

[14] Vattuone, L.; Savio, L.; Rocca, M. Bridging the structure gap: Chemistry of nanostructured surfaces at well-defined defects. *Surf. Sci. Rep.* **2008**, *63*, 101–168.

[15] Freund, H. -J.; Bäumer, M.; Libuda, J.; Risse, T.; Rupprechter, G.; Shaikhutdinov, S. Preparation and characterization of model catalysts: From ultrahigh vacuum to *in situ* conditions at the atomic dimension. *J. Catal.* **2003**, *216*, 223–235.

[16] Schnadt, J.; Rauls, E.; Xu, W.; Vang, R. T.; Knudsen, J.; Lægsgaard, E.; Li, Z.; Hammer, B.; Besenbacher, F. Extended one-dimensional supramolecular assembly on a stepped surface. *Phys. Rev. Lett.* **2008**, *100*, 046103.

[17] Besenbacher, F. Scanning tunnelling microscopy studies of metal surfaces. *Rep. Prog. Phys.* **1996**, *59*, 1737–1802.

[18] Uggerhøj, E. The Aarhus storage ring—A research facility for physics, chemistry, medicine, and materials sciences. *Nucl. Instrum. Meth. Phys. Res. B* **1995**, *99*, 261–266.

[19] McQuaide, B. H.; Banna, M. S. The core binding energies of some gaseous aromatic carboxylic acids and their relationship to proton affinities and gas phase acidities. *Can. J. Chem.* **1988**, *66*, 1919–1922.

[20] Patthey, L.; Rensmo, H.; Persson, P.; Westermark, K.; Vayssieres, L.; Stashans, A.; Petersson, Å.; Brühwiler, P. A.; Siegbahn, H.; Lunell, S.; Mårtensson, N. Adsorption of bi-isonicotinic acid on rutile TiO_2(110). *J. Chem. Phys.* **1999**, *110*, 5913–5918.

[21] Aplincourt, P.; Bureau, C.; Anthoine, J. -L.; Chong, D. P. Accurate density functional calculations of core electron binding energies on hydrogen-bonded systems. *J. Phys. Chem. A* **2001**, *105*, 7364–7370.

[22] Schnadt, J.; O'Shea, J. N.; Patthey, L.; Schiessling, J.; Krempaský, J.; Shi, M.; Mårtensson, N.; Brühwiler, P. A. Structural study of adsorption of isonicotinic acid and related molecules on rutile TiO_2(110) II: XPS. *Surf. Sci.* **2003**, *544*, 74–86.

[23] O'Shea, J. N.; Schnadt, J.; Brühwiler, P. A.; Hillesheimer, H.; Mårtensson, N.; Patthey, L.; Krempaský, J.; Wang, C. K.; Luo, Y.; Ågren, H. Hydrogen-bond induced surface core-level shift in isonicotinic acid. *J. Phys. Chem. B* **2001**, *105*, 1917–1920.

[24] O'Shea, J. N.; Luo, Y.; Schnadt, J.; Patthey, L.; Hillesheimer, H.; Krempaský, J.; Nordlund, D.; Nagasano, M.; Brühwiler, P. A.; Mårtensson, N. Hydrogen-bond induced surface core-level shift in pyridine carboxylic acids. *Surf. Sci.* **2001**, *486*, 157–166.

[25] Tabayahi, K.; Yamamoto, K.; Takahashi, O.; Tamenori, Y.; Harries, J. R.; Gejo, T.; Iseda, M.; Tamura, T.; Honma, K.; Suzuki, I. H.; Nagaoka, S.; Ibuki, T. Inner-shell excitation spectroscopy and fragmentation of small hydrogen-bonded clusters of formic acid after core excitations at the oxygen K edge. *J. Chem. Phys.* **2006**, *125*, 194307.

[26] Takahashi, O.; Yamanouchi, S.; Yamamoto, K.; Tabayashi, K. Theoretical study of the X-ray absorption spectra of small formic acid clusters. *Chem. Phys. Lett.* **2006**, *419*, 501–505.

[27] Minkov, I.; Gel'mukhanov, F.; Friedlein, R.; Osikowicz, W.; Suess, C.; Öhrwall, G.; Sorensen, S. L.; Braun, S.; Murdey, R.; Salaneck, W. R.; Ågren, H. Core excitations of naphthalene: Vibrational structure versus chemical shifts. *J. Chem. Phys.* **2004**, *121*, 5733–5739.

[28] Schnadt, J.; Schiessling, J.; O'Shea, J. N.; Gray, S. M.; Patthey, L.; Johansson, M. K. -J.; Shi, M.; Krempaský, J.; Åhlund, J.; Karlsson, P. G.; Persson, P.; Mårtensson, N.; Brühwiler, P. A. Structural study of adsorption of isonicotinic acid and related molecules on rutile TiO_2(110) I: XAS and STM. *Surf. Sci.* **2003**, *540*, 39–54.

[29] Kaduk, J. A.; Golab, J. T. Structures of 2,6-disubstituted naphthalenes. *Acta Crystallogr. B* **1999**, *55*, 85–94.

[30] Atodiresei, N.; Caciuc, V.; Franke, J. -H.; Blügel, S. Role of the van der Waals interactions on the bonding mechanism of pyridine on Cu(110) and Ag(110) surface: First-principles study. *Phys. Rev. B* **2008**, *78*, 045411.

[31] Jeffrey, G. A. *An Introduction to Hydrogen Bonding*; Oxford University Press: New York, 1997; p. 12.

[32] Tan, X.; Yang, G. W. Supramolecular nanowires self-assembly on stepped Ag(110) surface. *J. Phys. Chem. C* **2009**, *113*, 19926–19929.

[33] Pai, W. W.; Bartelt, N. C.; Peng, M. R.; Reutt-Robey, J. E. Steps as adatom sources for surface chemistry: oxygen overlayer formation on Ag(110). *Surf. Sci.* **1995**, *330*, L679–L685.

[34] Zambelli, T.; Barth, J. V.; Wintterlin, J. Formation mechanism of the O-induced added-row reconstruction on Ag(110): A low-temperature STM study. *Phys. Rev. B* **1998**, *58*, 12663–12666.

[35] Barth, J. V.; Weckesser, J.; Lin, N.; Dmitriev, A.; Kern, K. Supramolecular architectures and nanostructures at metal surfaces. *Appl. Phys. A* **2003**, *76*, 645–652.

[36] Lin, N.; Dmitriev, A.; Weckesser, J.; Barth, J. V.; Kern, K. Real-time single-molecule imaging of the formation and dynamics of coordination compounds. *Angew. Chem. Int. Ed.* **2002**, *41*, 4779–4783.

[37] Chen, Q.; Perry, C. C.; Frederick, B. G.; Murray, P. W.; Haq, S.; Richardson, N. V. Structural aspects of the

low-temperature deprotonation of benzoic acid on Cu(110) surfaces. *Surf. Sci.* **2000**, *446*, 63–75.

[38] Dougherty, D. B.; Maksymovych, P.; Yates, J. T. Direct STM evidence for Cu-benzoate surface complexes on Cu(110). *Surf. Sci.* **2006**, *600*, 4484–4491.

[39] Perry, C. C.; Haq, S.; Frederick, B. G.; Richardson, N. V. Face specificity and the role of metal adatoms in molecular reorientation at surfaces. *Surf. Sci.* **1998**, *409*, 512–520.

[40] Classen, T.; Lingenfelder, M.; Wang, Y.; Chopra, R.; Virojanadara, C.; Starke, U.; Costantini, G.; Fratesi, G.; Fabris, S.; de Gironcoli, S.; Baroni, S.; Haq, S.; Raval, R.; Kern, K. Hydrogen and coordination bonding supramolecular structures of trimesic acid on Cu(110). *J. Phys. Chem. A* **2007**, *111*, 12589–12603.

[41] Puschmann, A.; Haase, J.; Crapper, M. D.; Riley, C. E.; Woodruff, D. P. Structure determination of the formate intermediate on Cu(110) by use of X-ray absorption fine-structure measurements. *Phys. Rev. Lett.* **1985**, *54*, 2250–2252.

[42] Pascal, M.; Lamont, C. L. A; Kittel, M.; Hoeft, J. T.; Terborg, R.; Polcik, M.; Kang, J. H.; Toomes, R.; Woodruff, D. P. Quantitative structural determination of the high coverage phase of the benzoate species on Cu(110). *Surf. Sci.* **2001**, *492*, 285–293.

[43] Gomes, J. R. B.; Gomes, J. A. N. F. Adsorption of the formate species on copper surfaces: A DFT study. *Surf. Sci.* **1999**, *432*, 279–290.

[44] Casarin, M.; Maccato, C.; Vittadini, A. LCAO-LDA study of the chemisorption of formate on Cu(110) and Ag(110) surfaces. *J. Chem. Soc., Faraday Trans.* **1998**, *94*, 797–804.

[45] Lennartz, M. C.; Atodiresei, N.; Müller-Meskamp, L. M.; Karthäuser, S.; Waser, R.; Blügel, S. Cu-adatom-mediated bonding in close-packed benzoate/Cu(110) systems. *Langmuir* **2009**, *25*, 856–864.

[46] Montoya, A.; Haynes, B. S. DFT analysis of the reaction paths of formaldehyde decomposition on silver. *J. Phys. Chem. A* **2009**, *113*, 8125–8131.